INTERNATIONAL JOURNAL OF
NUMERICAL ANALYSIS AND MODELING
Volume 17, Number 6, Pages 839–857

CONNECTION BETWEEN GRAD-DIV STABILIZED STOKES FINITE ELEMENTS AND DIVERGENCE-FREE STOKES FINITE ELEMENTS

MICHAEL NEILAN AND AHMED ZYTOON

Abstract. In this paper, we use recently developed theories of divergence–free finite element schemes to analyze methods for the Stokes problem with grad-div stabilization. For example, we show that, if the polynomial degree is sufficiently large, the solutions of the Taylor–Hood finite element scheme converges to an optimal convergence exactly divergence–free solution as the grad-div parameter tends to infinity. In addition, we introduce and analyze a stable first-order scheme that does not exhibit locking phenomenon for large grad-div parameters.

Key words. Finite element methods, grad-div stabilization, divergence-free.

1. Introduction

Grad-div stabilization is a well-known and simple stabilization technique in numerical discretizations to improve mass conservation in simulations of incompressible flow. In its simplest form, the methodology adds the consistent term (written in strong form)

$$-\gamma\nabla(\nabla\cdot\boldsymbol{u})$$

to the momentum equations of the (Navier-)Stokes equations. Here, $\gamma > 0$ is a user-defined constant, which is referred to as the grad-div parameter. In addition to improving conservation of mass of the scheme, this stabilization technique may also improve the coupling errors of the velocity and pressure solutions. This can be advantageous for situations with large pressure gradients, e.g., in natural convection problems.

While enjoying many benefits, the use of grad-div stabilization comes with several practical disadvantages. These include a deterioration of the condition number and reduced sparsity of the algebraic system. Another disadvantage is the possible emergence of 'locking' for large grad-div parameters. Indeed, simply energy arguments show the discrete velocity solution satisfies $\|\nabla\cdot\boldsymbol{u}_h\| = O(\gamma^{-1})$, and therefore, in the limiting case, the discrete solution is divergence–free. If the discrete divergence–free subspace does not have rich enough approximation properties, then grad-div stabilization, while improving mass conservation, may lead to poor approximations.

The stability and convergence analysis for grad-div stabilization for incompressible flow have been explored in, e.g., [23, 9, 10, 27, 1]. These estimates, together with numerical simulations, provide a guide to choose optimal γ-values. For example, references [24, 21, 23, 4] suggests $\gamma = O(1)$ as the optimal value. On the other hand, numerical experiments in [12] and the analysis in [27, 1] suggest that the optimal choice may be much larger and depend on the finite element spaces, the mesh, and/or the viscosity of the model.

Received by the editors June 17, 2020 and, in revised form, September 11, 2020.
2000 *Mathematics Subject Classification.* 65N30, 65N15.

In another direction, and the path taken in this paper, is to identify and characterize the limiting solution as the grad-div parameter tends to infinity. For example, in [7, 19], it is shown that the Taylor–Hood finite element scheme on special (Clough-Tocher) triangulations, no locking occurs in the limiting case $\gamma \to \infty$, and the Taylor–Hood grad-div solution converges to the analogous (divergence–free) Scott–Vogelius solution.

The purpose of this paper is to extend and generalize the results in [7] by incorporating the recent theories of divergence–free finite element Stokes pairs. In this regard, we make two main contributions. First we show the absence of locking for the two-dimensional Taylor–Hood pair for a general class of meshes. In particular, we show that high–order Taylor–Hood pairs are generally locking-free. In addition, we show that the limiting (Taylor-Hood) solutions converge to the solution of the divergence–free Scott-Vogelius scheme, defined on general triangulations. The second contribution of the paper is the introduction and analysis of a new low–order and stable finite element pair that is locking–free. The velocity space is simply the linear Lagrange finite element space, and the pressure space consists of piecewise constants with respect to an auxiliary coarsened mesh.

The paper is organized as follows. In the next section, we introduce the notation and a framework for the grad-div finite element method for the Stokes problem. We show that the discrete solutions converge to a solution of a divergence–free method with rate $O(\gamma^{-1})$. In Section 3, we apply this framework to the two-dimensional Taylor–Hood elements. The general theme of the results is that additional mesh constraints are imposed for lower degree polynomial spaces. In Section 4, we define a stable first-order scheme for the Stokes problem, and show that the solutions converge to a divergence–free method as $\gamma \to \infty$. Finally, in Section 5 we provide some numerical experiments.

2. Notation and Framework

The Stokes equations defined on a polytope domain $\Omega \subset \mathbb{R}^d$ $(d = 2, 3)$ with Lipschitz continuous boundary $\partial\Omega$ is given by the system of equations

$$-\mu\Delta \boldsymbol{u} + \nabla p = \boldsymbol{f} \qquad \text{in } \Omega, \tag{1a}$$

$$\nabla \cdot \boldsymbol{u} = 0 \qquad \text{in } \Omega, \tag{1b}$$

$$\boldsymbol{u} = 0 \qquad \text{on } \partial\Omega, \tag{1c}$$

where the $\boldsymbol{u}$ is the velocity, p the pressure, and ∇, Δ denote the gradient operator and vector Laplacian operators, respectively. In (1a), μ is the viscosity.

We define the following function spaces on Ω:

$$L^2(\Omega) := \{w : \Omega \mapsto \mathbb{R} : \ \|w\|_{L^2(\Omega)} := (\int_\Omega |w|^2\,dx)^{1/2} < \infty\},$$

$$H^m(\Omega) := \{w : \Omega \mapsto \mathbb{R} : \ \|w\|_{H^m(\Omega)} := (\sum_{|\beta|\le m} \|D^\beta w\|^2_{L^2(\Omega)})^{1/2} < \infty\},$$

and set $(\cdot,\cdot)$ denote the inner product on $L^2(\Omega)$ and set $\|\cdot\| = \|\cdot\|_{L^2(\Omega)}$. The analogous spaces with boundary conditions are given by

$$L^2_0(\Omega) := \{w \in L^2(\Omega) : \ \int_\Omega w\,dx = 0\},$$

$$H^m_0(\Omega) := \{w \in H^m(\Omega) : \ D^\beta w|_{\partial\Omega} = 0, \forall \beta : \ |\beta| \le m-1\}.$$

We denote the analogous vector-valued function spaces in boldface; for example $\boldsymbol{H}^1(\Omega) = H^1(\Omega)^d$ and $\boldsymbol{L}^2(\Omega) = L^2(\Omega)^d$. We also define the space of $\boldsymbol{H}^1_0(\Omega)$

divergence–free vector fields

$$\boldsymbol{V} := \{\boldsymbol{v} \in \boldsymbol{H}_0^1(\Omega) : \nabla \cdot \boldsymbol{v} \equiv 0\}.$$

The weak formulation for (1) reads: Find $(\boldsymbol{u}, p) \in \boldsymbol{H}_0^1(\Omega) \times L_0^2(\Omega)$ such that $\forall(\boldsymbol{v}, q) \in \boldsymbol{H}_0^1(\Omega) \times L_0^2(\Omega)$ we have

$$\mu(\nabla \boldsymbol{u}, \nabla \boldsymbol{v}) - (\nabla \cdot \boldsymbol{v}, p) = (\boldsymbol{f}, \boldsymbol{v}), \tag{2a}$$

$$(\nabla \cdot \boldsymbol{u}, q) = 0. \tag{2b}$$

It is well known that the problem (2) has a unique solution [13].

Let $\boldsymbol{X}_h \times Y_h \subset \boldsymbol{H}_0^1(\Omega) \times L_0^2(\Omega)$ be a conforming finite element pair with respect to mesh parameter $h > 0$. For each such a pair, we define the space of discretely divergence–free vector fields as follows

$$\boldsymbol{V}_h := \{\boldsymbol{v} \in \boldsymbol{X}_h : (\nabla \cdot \boldsymbol{v}, q_h) = 0, \forall q_h \in Y_h\}.$$

We note, for many finite element pairs, there holds the non–inclusion $\boldsymbol{V}_h \not\subset \boldsymbol{V}$.

The discrete Stokes problem corresponding to the pair $\boldsymbol{X}_h \times Y_h$ reads: Find $(\boldsymbol{u}_h, p_h) \in \boldsymbol{X}_h \times Y_h$ such that $\forall(\boldsymbol{v}, q) \in \boldsymbol{X}_h \times Y_h$ we have

$$\mu(\nabla \boldsymbol{u}_h, \nabla \boldsymbol{v}) - (\nabla \cdot \boldsymbol{v}, p_h) = (\boldsymbol{f}, \boldsymbol{v}), \tag{3a}$$

$$(\nabla \cdot \boldsymbol{u}_h, q) = 0. \tag{3b}$$

Problem (3) has a unique solution provided that the pair $\boldsymbol{X}_h \times Y_h$ satisfies the inf-sup condition, that is, there exists a constant $\beta > 0$ independent of the mesh parameter h such that

$$\sup_{\boldsymbol{v} \in \boldsymbol{X}_h \setminus \{0\}} \frac{(\nabla \cdot \boldsymbol{v}, q)}{\|\nabla \boldsymbol{v}\|} \geq \beta \|q\| \qquad \forall q \in Y_h. \tag{4}$$

We introduce the corresponding grad-div stabilized problem, which reads: For given $\gamma \in \mathbb{R}$ with $\gamma > 0$, find $(\boldsymbol{u}_h^\gamma, p_h^\gamma) \in \boldsymbol{X}_h \times Y_h$ such that $\forall(\boldsymbol{v}, q) \in \boldsymbol{X}_h \times Y_h$ we have

$$\mu(\nabla \boldsymbol{u}_h^\gamma, \nabla \boldsymbol{v}) + \gamma(\nabla \cdot \boldsymbol{u}_h^\gamma, \nabla \cdot \boldsymbol{v}) - (\nabla \cdot \boldsymbol{v}, p_h^\gamma) = (\boldsymbol{f}, \boldsymbol{v}), \tag{5a}$$

$$(\nabla \cdot \boldsymbol{u}_h^\gamma, q) = 0. \tag{5b}$$

Again, standard arguments show that (5) is well-posed provided the inf-sup condition (4) is satisfied. Adding the term $\gamma(\nabla \cdot \boldsymbol{u}_h^\gamma, \nabla \cdot \boldsymbol{v}_h)$ improves mass conservation and can reduce the effect of the pressure error on the velocity approximation. The limiting case $\gamma \to \infty$ is studied in the following two theorems.

Theorem 2.1. *Let $\boldsymbol{X}_h \times Y_h$ be a conforming finite element pair defined satisfying the inf-sup condition. Let $\{\gamma_i\}_{i=1}^\infty \subset \mathbb{R}$ with $\gamma_i \to \infty$, and let $(\boldsymbol{u}_i, p_i) \in \boldsymbol{X}_h \times Y_h$ be the solution for* (5) *corresponding to γ_i. Then the sequence $\{\boldsymbol{u}_i\}_{i=1}^\infty \subset \boldsymbol{X}_h$ converges to some $\boldsymbol{w}_h \in \boldsymbol{X}_h \cap \boldsymbol{V}$. Moreover,*

$$\|\nabla(\boldsymbol{u} - \boldsymbol{w}_h)\| = \inf_{\boldsymbol{v} \in \boldsymbol{X}_h \cap \boldsymbol{V}} \|\nabla(\boldsymbol{u} - \boldsymbol{v})\|. \tag{6}$$

Proof. We follow the ideas in [7, Theorem 3.1] and begin with an a priori bound which is obtained by taking $\boldsymbol{v} = \boldsymbol{u}_i$ and $q = p_i$ in (5):

$$\mu\|\nabla \boldsymbol{u}_i\|^2 + \gamma_i\|\nabla \cdot \boldsymbol{u}_i\|^2 = |(\boldsymbol{f}, \boldsymbol{u}_i)|. \tag{7}$$

Thus, we have the following inequality

$$\mu\|\nabla \boldsymbol{u}_i\| \leq \|\boldsymbol{f}\|_{*,h} \quad \forall i \in \mathbb{N},$$

where $\|\boldsymbol{f}\|_{*,h} = \sup_{\boldsymbol{v}\in\boldsymbol{X}_h\setminus\{0\}} \frac{|(\boldsymbol{f},\boldsymbol{v})|}{\|\nabla \boldsymbol{v}\|}$. The above inequality shows that the sequence $\{\boldsymbol{u}_i\}_{i=1}^{\infty}$ is a uniformly bounded sequence in the finite dimensional space $\boldsymbol{X}_h$. Hence, $\{\boldsymbol{u}_i\}_{i=1}^{\infty}$ has a convergent subsequence $\{\boldsymbol{u}_{i_j}\}_j$ that converges to some $\boldsymbol{w}_h \in \boldsymbol{X}_h$.

To show $\boldsymbol{w}_h \in \boldsymbol{V}$, i.e., $\nabla\cdot\boldsymbol{w}_h = 0$, we use (7) and the Cauchy-Schwarz inequality to obtain

$$\|\nabla\cdot\boldsymbol{u}_{i_j}\| \le \frac{1}{\sqrt{2\mu\gamma_{i_j}}}\|\boldsymbol{f}\|_{*,h} \quad \forall j\in\mathbb{N}. \tag{8}$$

Because $\|\nabla\cdot\boldsymbol{v}\| \le \sqrt{2}\|\nabla\boldsymbol{v}\|$ for all $\boldsymbol{v}\in\boldsymbol{H}_0^1(\Omega)$ and $\boldsymbol{u}_{i_j}\to\boldsymbol{w}_h$, it follows that

$$\begin{aligned}\|\nabla\cdot\boldsymbol{w}_h\| &= \|\nabla\cdot(\boldsymbol{w}_h - \boldsymbol{u}_{i_j} + \boldsymbol{u}_{i_j})\| \\ &\le \|\nabla\cdot(\boldsymbol{w}_h - \boldsymbol{u}_{i_j})\| + \|\nabla\cdot\boldsymbol{u}_{i_j}\| \\ &\le \sqrt{2}\|\nabla(\boldsymbol{w}_h - \boldsymbol{u}_{i_j})\| + \frac{1}{\sqrt{2\mu\gamma_{i_j}}}\|\boldsymbol{f}\|_{*,h} \to 0 \text{ as } j\to\infty.\end{aligned}$$

Hence, we conclude that $\|\nabla\cdot\boldsymbol{w}_h\| = 0$, and so $\boldsymbol{w}_h\in\boldsymbol{V}$.

To show the estimate (6) and the uniqueness of $\boldsymbol{w}_h$, we observe that for $\boldsymbol{v}\in \boldsymbol{X}_h\cap\boldsymbol{V}$ we have

$$\begin{aligned}\mu(\nabla\boldsymbol{w}_h,\nabla\boldsymbol{v}) - (\boldsymbol{f},\boldsymbol{v}) &= \lim_{j\to\infty}\mu(\nabla\boldsymbol{u}_{i_j},\nabla\boldsymbol{v}) + \lim_{j\to\infty}\gamma_{i_j}(\nabla\cdot\boldsymbol{u}_{i_j},\nabla\cdot\boldsymbol{v}) - (\boldsymbol{f},\boldsymbol{v}) \\ &= \lim_{j\to\infty}\left(\mu(\nabla\boldsymbol{u}_{i_j},\nabla\boldsymbol{v}) + \gamma_{i_j}(\nabla\cdot\boldsymbol{u}_{i_j},\nabla\cdot\boldsymbol{v}) - (\boldsymbol{f},\boldsymbol{v})\right) \\ &= 0.\end{aligned}$$

Hence, $\boldsymbol{w}_h$ satisfies

$$\mu(\nabla\boldsymbol{w}_h,\nabla\boldsymbol{v}) = (\boldsymbol{f},\boldsymbol{v}) \qquad \forall\boldsymbol{v}\in\boldsymbol{X}_h\cap\boldsymbol{V}, \tag{9}$$

and (6) immediately follows by Cea's lemma.

By the Lax-Milgram theorem, problem (9) has a unique solution. If $\{\boldsymbol{u}_{i_k}\}_k$ is another convergent subsequence of $\{\boldsymbol{u}_i\}_{i=1}^{\infty}$ that converges to some $\boldsymbol{z}_h\in\boldsymbol{X}_h$, then $\boldsymbol{z}_h$ is a solution to the problem (9). Since the problem (9) has a unique solution, we conclude that $\boldsymbol{w}_h = \boldsymbol{z}_h$, which means any convergent subsequence of $\{\boldsymbol{u}_i\}_{i=1}^{\infty}$ converges to the same element in $\boldsymbol{X}_h$. Hence the entire sequence $\{\boldsymbol{u}_i\}_{i=1}^{\infty}$ converges to $\boldsymbol{w}_h$. □

Theorem 2.2. *Suppose that the conditions of Theorem 2.1 are satisfied. Set*

$$Q_h := \nabla\cdot\boldsymbol{X}_h = \{\nabla\cdot\boldsymbol{v} :\ \boldsymbol{v}\in\boldsymbol{X}_h\},$$

and suppose that $Y_h\subset Q_h$ and $\boldsymbol{X}_h\times Q_h$ is an inf-sup stable pair, i.e.,

$$\sup_{\boldsymbol{v}\in\boldsymbol{X}_h\setminus\{0\}}\frac{(\nabla\cdot\boldsymbol{v},q)}{\|\nabla\boldsymbol{v}\|} \ge \beta_Q\|q\| \qquad \forall q\in Q_h, \quad \exists\beta_Q>0. \tag{10}$$

Then the sequence $\{(\boldsymbol{u}_i, p_i - \gamma_i\nabla\cdot\boldsymbol{u}_i)\}_{i=1}^{\infty}\subset\boldsymbol{X}_h\times Q_h$ converges to $(\boldsymbol{w}_h,p_h)\in(\boldsymbol{X}_h\cap\boldsymbol{V})\times Q_h$ satisfying

$$\mu(\nabla\boldsymbol{w}_h,\nabla\boldsymbol{v}) - (\nabla\cdot\boldsymbol{v},p_h) = (\boldsymbol{f},\boldsymbol{v}) \qquad \forall\boldsymbol{v}\in\boldsymbol{X}_h, \tag{11a}$$

$$(\nabla\cdot\boldsymbol{w}_h,q) = 0 \qquad \forall q\in Q_h. \tag{11b}$$

There also holds

(12)
$$\begin{aligned}\beta_Q^2\mu^{-1}\|p_h - (p_i - \gamma_i\nabla\cdot\boldsymbol{u}_i)\| &\le \beta_Q\|\nabla(\boldsymbol{w}_h - \boldsymbol{u}_i)\| \\ &\le \|\nabla\cdot\boldsymbol{u}_i\| \le \min\{2\beta_Q^{-1}\gamma_i^{-1},(2\mu\gamma_i)^{-1/2}\}\|\boldsymbol{f}\|_{*,h}.\end{aligned}$$

Proof. The convergence $\boldsymbol{u}_i \to \boldsymbol{w}_h$ for some $\boldsymbol{w}_h \in \boldsymbol{X}_h \cap \boldsymbol{V}$ is established in Theorem 2.1. Since $\boldsymbol{w}_h$ is divergence–free, it clearly satisfies (11b).

To show the convergence of the modified pressure sequence, we first use with the inf-sup condition for the pair $\boldsymbol{X}_h \times Q_h$ (10) and the inclusion $Y_h \subset Q_h$ to obtain

$$\begin{aligned}\beta_Q \|p_i - \gamma_i \nabla \cdot \boldsymbol{u}_i\| &\leq \sup_{\boldsymbol{v} \in \boldsymbol{X}_h \setminus \{0\}} \frac{-(\nabla \cdot \boldsymbol{v}, p_i) + \gamma_i (\nabla \cdot \boldsymbol{u}_i, \nabla \cdot \boldsymbol{v})}{\|\nabla \boldsymbol{v}\|} \\ &= \frac{(\boldsymbol{f}, \boldsymbol{v}) - \mu(\nabla \boldsymbol{u}_i, \nabla \boldsymbol{v})}{\|\nabla \boldsymbol{v}\|} \leq \|\boldsymbol{f}\|_{*,h} + \mu \|\nabla \boldsymbol{u}_i\|.\end{aligned}$$

Thus, $\{p_i - \gamma_i \nabla \cdot \boldsymbol{u}_i\}_{i=1}^{\infty} \subset Q_h$ is a bounded sequence, and thus has a convergent subsequence: $p_{i_j} - \gamma_{i_j} \nabla \cdot \boldsymbol{u}_{i_j} \to p_h$ for some $p_h \in Q_h$. We then find that, for any $\boldsymbol{v} \in \boldsymbol{X}_h$,

$$\begin{aligned}(\nabla \boldsymbol{w}_h, \nabla \boldsymbol{v}) - (\nabla \cdot \boldsymbol{v}, p_h) &= \lim_{j \to \infty} \big((\nabla \boldsymbol{u}_{i_j}, \nabla \boldsymbol{v}) - (p_{i_j}, \nabla \cdot \boldsymbol{v}) + \gamma_{i_j} (\nabla \cdot \boldsymbol{u}_{i_j}, \nabla \cdot \boldsymbol{v}) \big) \\ &= (\boldsymbol{f}, \boldsymbol{v}).\end{aligned}$$

We conclude that $(\boldsymbol{w}_h, p_h) \in \boldsymbol{X}_h \times Q_h$ satisfies (11). The convergence of the entire sequence $\{(\boldsymbol{u}_i, p_i - \gamma_i \nabla \cdot \boldsymbol{u}_i)\}_{i=1}^{\infty}$ follows directly from the arguments in Theorem 2.1.

Next we establish the rate of convergence given in (12). As a first step, we first note that $\|\nabla \boldsymbol{w}_h\| \leq \mu^{-1} \|f\|_{*,h}$. Consequently, by the inf–sup condition (10),

$$(13)\quad \beta_Q \|p_h\| \leq \sup_{\boldsymbol{v} \in \boldsymbol{X}_h \setminus \{0\}} \frac{(\nabla \cdot \boldsymbol{v}, p_h)}{\|\nabla \boldsymbol{v}\|} = \sup_{\boldsymbol{v} \in \boldsymbol{X}_h \setminus \{0\}} \frac{(\boldsymbol{f}, \boldsymbol{v}) - \mu(\nabla \boldsymbol{w}_h, \nabla \boldsymbol{v})}{\|\nabla \boldsymbol{v}\|} \leq 2\|\boldsymbol{f}\|_{*,h}.$$

Write $\boldsymbol{e}_i = \boldsymbol{w}_h - \boldsymbol{u}_i \in \boldsymbol{V}_h$ and note that

$$(14)\qquad \mu(\nabla \boldsymbol{e}_i, \nabla \boldsymbol{v}) - (p_h - p_i, \nabla \cdot \boldsymbol{v}) + \gamma_i (\nabla \cdot \boldsymbol{e}_i, \nabla \cdot \boldsymbol{v}) = 0 \qquad \forall \boldsymbol{v} \in \boldsymbol{X}_h.$$

Consequently, by setting $\boldsymbol{v} = \boldsymbol{e}_i$ and using $\nabla \cdot \boldsymbol{w}_h = 0$, we find

$$\mu \|\nabla \boldsymbol{e}_i\|^2 + \gamma_i \|\nabla \cdot \boldsymbol{u}_i\|^2 = (\nabla \cdot \boldsymbol{e}_i, p_h - p_i) = (\nabla \cdot \boldsymbol{e}_i, p_h) \leq \|\nabla \cdot \boldsymbol{u}_i\| \|p_h\|.$$

Therefore by (13),

$$\|\nabla \cdot \boldsymbol{u}_i\| \leq \frac{2}{\gamma_i \beta_Q} \|\boldsymbol{f}\|_{*,h}.$$

Combined with (8), this establishes the last inequality in (12).

To derive a convergence rate for $\|\nabla \boldsymbol{e}_i\|$ with respect to γ_i, we introduce the space

$$\boldsymbol{R}_h = (\boldsymbol{X}_h \cap \boldsymbol{V})^{\perp} = \{\boldsymbol{v} \in \boldsymbol{X}_h : \ (\nabla \boldsymbol{v}, \nabla \boldsymbol{w}) = 0 \ \forall \boldsymbol{w} \in \boldsymbol{X}_h \cap \boldsymbol{V}\}.$$

Because $\boldsymbol{X}_h \cap \boldsymbol{V} = \{\boldsymbol{v} \in \boldsymbol{X}_h : \ (\nabla \cdot \boldsymbol{v}, q) = 0 \ \forall q \in Q_h\}$, and $\boldsymbol{X}_h \times Y_h$ is assumed to be inf-sup stable, there holds [20]

$$(15)\qquad \|\nabla \boldsymbol{v}\| \leq \beta_Q^{-1} \|\nabla \cdot \boldsymbol{v}\| \qquad \forall \boldsymbol{v} \in \boldsymbol{R}_h.$$

Write $\boldsymbol{e}_i = \boldsymbol{e}_i^0 + \boldsymbol{e}_i^R$ with $\boldsymbol{e}_i^0 \in \boldsymbol{X}_h \cap \boldsymbol{V}$ and $\boldsymbol{e}_i^R \in \boldsymbol{R}_h$. Because $\|\nabla \boldsymbol{e}_i\|^2 = \|\nabla \boldsymbol{e}_i^0\|^2 + \|\nabla \boldsymbol{e}^R\|^2$ and $\nabla \cdot \boldsymbol{e}_i^0 = 0$, there holds by (15)

$$\|\nabla \boldsymbol{e}_i^R\| \leq \beta_Q^{-1} \|\nabla \cdot \boldsymbol{e}_i^R\| = \beta_Q^{-1} \|\nabla \cdot \boldsymbol{e}_i\| = \beta_Q^{-1} \|\nabla \cdot \boldsymbol{u}_i\|.$$

On the other hand, by taking $\boldsymbol{v} = \boldsymbol{e}_i^0 \in \boldsymbol{X}_h \cap \boldsymbol{V}$ in (14), we get

$$\begin{aligned}0 &= \mu(\nabla \boldsymbol{e}_i, \nabla \boldsymbol{e}_i^0) - (p_h - p_i, \nabla \cdot \boldsymbol{e}_i^0) + \gamma_i (\nabla \cdot \boldsymbol{e}_i, \nabla \cdot \boldsymbol{e}_i^0) \\ &= \mu(\nabla \boldsymbol{e}_i^R, \nabla \boldsymbol{e}_i^0) + \mu \|\nabla \boldsymbol{e}_i^0\|^2 = \mu \|\nabla \boldsymbol{e}_i^0\|^2.\end{aligned}$$

Thus $\boldsymbol{e}_i^0 \equiv 0$, and therefore

$$\|\nabla \boldsymbol{e}_i\| = \|\nabla \boldsymbol{e}_i^R\| \leq \beta_Q^{-1} \|\nabla \cdot \boldsymbol{u}_i\|.$$

Finally, we use the inf-sup condition on $\boldsymbol{X}_h \times Q_h$ to derive the convergence rate of the modified pressure equation as follows:

$$\begin{aligned}\beta_Q \|p_h - (p_i - \gamma_i \nabla\cdot \boldsymbol{u}_i)\| &\le \sup_{\boldsymbol{v}\in \boldsymbol{X}_h\backslash\{0\}} \frac{(\nabla\cdot\boldsymbol{v}, p_h) - (\nabla\cdot\boldsymbol{v}, p_i) + \gamma_i(\nabla\cdot\boldsymbol{u}_i, \nabla\cdot\boldsymbol{v})}{\|\nabla \boldsymbol{v}\|}\\ &= \sup_{\boldsymbol{v}\in \boldsymbol{X}_h\backslash\{0\}} \frac{-\mu(\nabla \boldsymbol{e}_i, \nabla\boldsymbol{v})}{\|\nabla\boldsymbol{v}\|} \le \mu\|\nabla \boldsymbol{e}_i\|.\end{aligned}$$

□

Remark 2.3. Since $\boldsymbol{w}_h \in \boldsymbol{X}_h \cap \boldsymbol{V}$, the error $\|\nabla(\boldsymbol{u}-\boldsymbol{u}_i)\|$ can be decomposed as follows

$$\begin{aligned}\|\nabla(\boldsymbol{u}-\boldsymbol{u}_i)\| &= \|\nabla(\boldsymbol{u}-\boldsymbol{w}_h+\boldsymbol{w}_h-\boldsymbol{u}_i)\|\\ &\le \|\nabla(\boldsymbol{u}-\boldsymbol{w}_h)\| + \|\nabla\boldsymbol{e}_i\|\\ &\le \inf_{\boldsymbol{v}\in\boldsymbol{V}\cap\boldsymbol{X}_h}\|\nabla(\boldsymbol{u}-\boldsymbol{v})\| + \frac{2}{\beta_Q^2\gamma_i}\|\boldsymbol{f}\|_{*,h}.\end{aligned}$$

Since the pair $\boldsymbol{X}_h \times Q_h$ is inf-sup stable, we have by [6, Theorem 12.5.17] to get the estimate

$$\|\nabla(\boldsymbol{u}-\boldsymbol{u}_i)\| \le \Big(1+\frac{C}{\beta_Q}\Big)\inf_{\boldsymbol{v}\in\boldsymbol{X}_h}\|\nabla(\boldsymbol{u}-\boldsymbol{v})\| + \frac{2}{\beta_Q^2\gamma_i}\|\boldsymbol{f}\|_{*,h}, \tag{16}$$

where $C>0$ is a constant independent of h, β_Q and γ_i.

For comparison, the following estimate for grad-div stabilized finite element methods for the Stokes problem was derived in [27]:

$$\|\nabla(\boldsymbol{u}-\boldsymbol{u}_i)\|^2 \le \inf_{\boldsymbol{v}\in\boldsymbol{V}_h}\Big(4\|\nabla(\boldsymbol{u}-\boldsymbol{v})\|^2 + 2\frac{\gamma_i}{\mu}\|\nabla\cdot\boldsymbol{v}\|^2\Big) + \frac{2}{\mu\gamma_i}\inf_{q_h\in Y_h}\|p_h-q_h\|^2, \tag{17}$$

Note that

$$\begin{aligned}\inf_{\boldsymbol{v}\in\boldsymbol{V}_h}\Big(4\|\nabla(\boldsymbol{u}-\boldsymbol{v})\|^2 + 2\frac{\gamma_i}{\mu}\|\nabla\cdot\boldsymbol{v}\|^2\Big) &\le \inf_{\boldsymbol{v}\in\boldsymbol{X}_h\cap\boldsymbol{V}}\Big(4\|\nabla(\boldsymbol{u}-\boldsymbol{v})\|^2 + 2\frac{\gamma_i}{\mu}\|\nabla\cdot\boldsymbol{v}\|^2\Big)\\ &\le \Big(1+\frac{C}{\beta_Q}\Big)\inf_{\boldsymbol{v}\in\boldsymbol{X}_h}\|\nabla(\boldsymbol{u}-\boldsymbol{v})\|\end{aligned}$$

for a generally different constant $C>0$. Thus, we see that the first term in the right-hand side of (17) is sharper than the analogous term in (16). On the other hand, unlike estimate (17), the bound (16) does not depend on μ. Thus, we conclude that the estimate (16) can be sharper than the estimate (17) for small values of μ.

3. Application I: Taylor–Hood Pairs

In this section, we apply Theorem 2.2 to the two–dimensional Taylor–Hood pair and show, under assumptions of the mesh and the polynomial degree, the Taylor–Hood finite element method with grad-div stabilization does not experience locking in the limit $\gamma\to\infty$. To proceed, we require some additional notation.

Denote by $\mathcal{T}_h$ a conforming, shape–regular, simplicial triangulation of $\Omega\subset\mathbb{R}^2$. For $T\in\mathcal{T}_h$, we denote by $h_T = \text{diam}(T)$ and set $h = \max_{T\in\mathcal{T}_h} h_T$. Let $\mathcal{V}_h^I$ and $\mathcal{V}_h^B$ denote the sets of interior and boundary vertices of $\mathcal{T}_h$, respectively, and set $\mathcal{V}_h = \mathcal{V}_h^I\cup\mathcal{V}_h^B$.

Let $\mathcal{P}_k(S)$ denote the space of polynomials of degree $\le k$ with domain S; the analogous vector-valued space is denoted by $\boldsymbol{\mathcal{P}}_k(S) := [\mathcal{P}_k(S)]^2$. We define the piecewise polynomials with respect to the mesh $\mathcal{T}_h$ as

$$\mathcal{P}_k(\mathcal{T}_h) := \prod_{T\in\mathcal{T}_h} \mathcal{P}_k(T).$$

For an integer $k \geq 2$, the Taylor–Hood pair is given as

$$\begin{aligned} \boldsymbol{X}_h^{TH} &= \boldsymbol{\mathcal{P}}_k(\mathcal{T}_h) \cap \boldsymbol{H}_0^1(\Omega), \\ Y_h^{TH} &= \mathcal{P}_{k-1}(\mathcal{T}_h) \cap H^1(\Omega) \cap L_0^2(\Omega). \end{aligned}$$

We also define the image of the divergence acting on the Taylor–Hood velocity space:

$$Q_h^{TH} := \nabla \cdot \boldsymbol{X}_h^{TH} = \{\nabla \cdot \boldsymbol{v} : \boldsymbol{v} \in \boldsymbol{X}_h^{TH}\}. \tag{18}$$

It is well known that the pair $\boldsymbol{X}^{TH} \times Y_h^{TH}$ is inf–sup stable provided that each $T \in \mathcal{T}_h$ has at most one boundary edge [5]. We assume this mild condition is satisfied throughout this section.

To apply Theorem 2.2 to the Taylor–Hood pair, we split the results into three cases, depending on the polynomial degree: $k \geq 4$, $k = 3$, and $k = 2$. The general theme is that additional mesh conditions are introduced for lower degree polynomial spaces.

3.1. High order pairs: $k \geq 4$. To apply Theorem 2.2 on the Taylor–Hood pair for $k \geq 4$, we need to establish the inf–sup stability of the pair $\boldsymbol{X}_h^{TH} \times Q_h^{TH}$. To do so, following the notation introduced in [16], we introduce the concept of a singular vertex and the vertex singularity of a mesh.

For $z \in \mathcal{V}_h$, let $\mathcal{T}_z \subset \mathcal{T}_h$ denote the set of triangles that have z as a vertex. We assume that $\mathcal{T}_z = \{T_1, \ldots, T_N\}$, enumerating such that T_j and T_{j+1} share an edge for $j = 1, \ldots, N-1$, and if z is an interior vertex, then T_1 and T_N share an edge. Letting θ_j denote the angle between the angle between the edges of T_j originating from z, we define

$$\Theta_z := \begin{cases} \max\{|\sin(\theta_1+\theta_2)|, \ldots |\sin(\theta_{N-1}+\theta_N)|, |\sin(\theta_1+\theta_N)|\} & \text{if } z \in \mathcal{V}_h^I, \\ \max\{|\sin(\theta_1+\theta_2)|, \ldots |\sin(\theta_{N-1}+\theta_N)|\} & \text{if } z \in \mathcal{V}_h^B. \end{cases}$$

Definition 3.1.

(i) We say that a vertex z is *singular* if $\Theta_z = 0$; otherwise we say that z is *non–singular.*

(ii) The *measure of vertex singularity* of the mesh is given by the positive number

$$\Theta_* := \min_{\substack{z\in\mathcal{V}_h \\ \Theta_z\neq 0}} \Theta_z > 0.$$

Remark 3.2. An interior vertex is singular if and only if exactly two straight lines emanating from the vertex (and hence $N = 4$ in this case). A non–corner boundary vertex z is singular if exactly two triangles have z as a vertex. Finally, a corner (boundary) vertex z is singular if only one triangle in $\mathcal{T}_h$ has z as a vertex. Note that, because we assumed that each $T \in \mathcal{T}_h$ has at most one boundary edge, there exists no corner singular vertices.

The quantity Θ_z gives an indication on "how close" a non–singular vertex z is from being singular. Essentially, if Θ_* is small, then there exists a vertex in $\mathcal{T}_h$ that is a small perturbation of a singular vertex. Note that if the cardinality of $\mathcal{T}_z$ is greater than 4 for all $z \in \mathcal{V}_h^I$, and greater than 2 for all $z \in \mathcal{V}_h^B$, then Θ_* is uniformly bounded from below.

Let

$$\mathcal{S}_h = \{z \in \mathcal{V}_h : \ \Theta_z = 0\}$$

denote the set of singular vertices in the mesh $\mathcal{T}_h$. A characterization of the divergence operator acting on the Taylor–Hood velocity space is given in the next lemma for high–order pairs. Its proof is found in [16, 26].

Lemma 3.3. *Suppose that $k \ge 4$. Then there holds*

$$Y_h^{TH} \subset Q_h^{TH} := \nabla \cdot \boldsymbol{X}_h^{TH} = \{q \in \mathcal{P}_{k-1}(\mathcal{T}_h) \cap L_0^2(\Omega) : \ \sum_{\ell=1}^{N} (-1)^\ell q|_{T_\ell}(z) = 0 \ \forall z \in \mathcal{S}_h\}.$$

Moreover, $\boldsymbol{X}_h^{TH} \times Q_h^{TH}$ represents an inf-sup stable pair with inf-sup constant β_Q independent of size of the triangles in $\mathcal{T}_h$. Rather, $\beta_Q = C\Theta_*$ for some h-independent constant $C > 0$.

Combining Lemma 3.3 with Theorem 2.2 then yields the convergence of the (high–order) grad-div stabilized Taylor–Hood pair.

Theorem 3.4. *Let $\{\gamma_i\}_{i=1}^\infty \subset \mathbb{R}$ with $\gamma_i \to \infty$ and $(\boldsymbol{u}_i, p_i) \in \boldsymbol{X}_h^{TH} \times Y_h^{TH}$ be the solution of the grad-div stabilized Stokes problem* (5) *corresponding to γ_i using the Taylor–Hood pair with $k \ge 4$. Then $\boldsymbol{u}_i \to \boldsymbol{w}_h$ and $p_i - \gamma_i \nabla \cdot \boldsymbol{u}_i \to p_h$ as $i \to \infty$ for some $\boldsymbol{w}_h \in \boldsymbol{X}_h^{TH} \cap \boldsymbol{V}$ and $p_h \in Q_h^{TH}$ with $(\boldsymbol{w}_h, p_h)$ being the solution for* (11) *with $\times Q_h = \boldsymbol{X}_h^{TH} \times Q_h^{TH}$. In particular,*

(19)
$$\Theta_* \mu^{-1} \|p_h - (p_i - \gamma_i \nabla \cdot \boldsymbol{u}_i)\| \le \|\nabla(\boldsymbol{w}_h - \boldsymbol{u}_i)\| \le C\Theta_*^{-1} \min\{\Theta_*^{-1}\gamma_i^{-1}, (\mu\gamma_i)^{-1/2}\},$$

where $C > 0$ is independent of h, μ, and Θ_*.

If $\boldsymbol{u} \in \boldsymbol{H}^s(\Omega)$ for some $s \ge 1$, then the divergence–free function $\boldsymbol{w}_h$ satisfies

$$\|\nabla(\boldsymbol{u} - \boldsymbol{w}_h)\| \le Ch^{\ell-1} \|\boldsymbol{u}\|_{H^\ell(\Omega)}, \tag{20}$$

where $\ell = \min\{k+1, s\}$ and $C > 0$ is independent of h, γ, μ and Θ_*.

Remark 3.5. For fixed μ, Theorem 3.4 implies that the convergence for the sequence $\{(\boldsymbol{u}_i, p_i - \gamma_i \nabla \cdot \boldsymbol{u}_i)\}_{i=1}^\infty$ to $(\boldsymbol{w}_h, p_h)$ is $O(\gamma_i^{-1})$ provided $\gamma_i \gtrsim \Theta_*^{-2}\mu$. Otherwise, for smaller grad-div parameters the theorem predicts $O(\gamma_i^{-1/2})$ convergence.

Remark 3.6. Theorem 3.4 states that $\{\boldsymbol{u}_i\}_{i=1}^\infty$ converges to an exactly divergence–free solution with optimal order properties as $i \to \infty$; this is true on meshes with singular vertices or "nearly singular" vertices.

Proof. The convergence and convergence rates for the sequence $\{(\boldsymbol{u}_i, p_i - \gamma_i \nabla \cdot \boldsymbol{u}_i)\}_{i=1}^\infty$ directly follow from Lemma 3.3 with Theorem 2.2.

To prove (20), we first use the estimate (6):

$$\|\nabla(\boldsymbol{u} - \boldsymbol{w}_h)\| \le \inf_{\boldsymbol{v} \in \boldsymbol{V} \cap \boldsymbol{X}_h} \|\nabla(\boldsymbol{u} - \boldsymbol{v})\|.$$

Following [11], we introduce the modified H^2-conforming Argyris (TUBA) finite element space [2]

$$\Sigma_h = \{s \in H_0^2(\Omega) \cap \mathcal{P}_{k+1}(\mathcal{T}_h) : \ s \text{ is } C^2 \text{ at all non-corner vertices of } \mathcal{T}_h\}.$$

We then have [11]

$$\nabla \times \Sigma_h := \{\nabla \times s : \ s \in \Sigma_h\} \subset \boldsymbol{V} \cap \boldsymbol{X}_h,$$

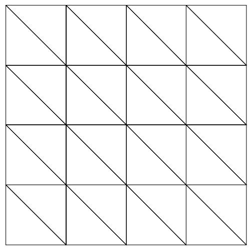

FIGURE 1. Type–I triangulation on $(0,1)^2$.

where $\nabla\times s = (\partial s/\partial x_2, -\partial s/\partial x_1)^\intercal$ is the two–dimensional curl operator. Therefore, by writing $\boldsymbol{u}$ in terms of its stream function $\boldsymbol{u} = \nabla\times\psi$ for some $\psi \in H_0^2(\Omega)\cap H^{s+1}(\Omega)$, we have

$$\begin{aligned}\inf_{\boldsymbol{v}\in \boldsymbol{V}\cap \boldsymbol{X}_h} \|\nabla(\boldsymbol{u}-\boldsymbol{v})\| &\le \inf_{\boldsymbol{v}\in\nabla\times\Sigma_h} \|\nabla(\boldsymbol{u}-\boldsymbol{v})\| \\ &= \inf_{s\in\Sigma_h} \|D^2(\psi - s)\| \le Ch^{\ell-1}\|\psi\|_{H^{\ell-1}(\Omega)} \le Ch^{\ell-1}\|\boldsymbol{u}\|_{H^\ell(\Omega)}.\end{aligned}$$

□

3.2. The cubic–quadratic Taylor–Hood pair. To apply Theorem 2.2 to the cubic-quadratic Taylor–Hood pair, we incorporate the recent stability results of the cubic-quadratic Scott–Vogelius pair in [17]. In particular, a characterization of the space Q_h^{TH} (cf. (18)) was explicitly given and inf–sup stability results were shown. To explain these results further, we introduce the concept of a interpolating vertex.

Recall that for a vertex $z\in\mathcal{V}_h$, $\mathcal{T}_z = \{T_1,\ldots,T_N\}$ denotes the set of triangles that have z as vertex. Set

$$\boldsymbol{W}_z := \{\boldsymbol{a}\in\mathbb{R}^N :\ \text{if } z\in\mathcal{S}_h, \text{ then } \sum_{j=1}^N (-1)^j a_j = 0\}.$$

Set

$$\Omega_z = \operatorname{int}\Big(\cup_{T\in\mathcal{T}_z} \bar{T}\Big),$$

and define

$$\begin{aligned}&\boldsymbol{X}_z \\ &=\{\boldsymbol{v}\in\boldsymbol{X}_h^{TH} :\ \operatorname{supp}\boldsymbol{v}\subset\Omega_z : \int_T \nabla\cdot\boldsymbol{v}\,dx = 0\ \forall T\in\mathcal{T}_h, (\nabla\cdot\boldsymbol{v})(\sigma) = 0\ \forall\sigma\in\mathcal{V}_h\backslash\{z\}\}.\end{aligned}$$

Definition 3.7. We say that $z\in\mathcal{V}_h$ is an *interpolating vertex* if, for all $\boldsymbol{a}\in\boldsymbol{W}_z$, there exists $\boldsymbol{v}\in\boldsymbol{X}_z$ such that $(\nabla\cdot\boldsymbol{v})|_{T_j}(z) = a_j$ for all $j\in\{1,2,\ldots,N\}$. We denote the set of all interpolating vertices in $\mathcal{V}_h$ by $\mathcal{L}_h$.

Remark 3.8. examples are given in [17], where the local interpolating vertex property in Definition 3.7 is satisfied by all interior vertices. Examples include

(1) Criss-crossed mesh
(2) Every mesh $\mathcal{T}_h$ such that $|\mathcal{T}_z| = N$ is odd for all $z\in\mathcal{V}_h^I$.

It is also shown in [17] that not every interior vertex in a type–I triangulation (cf. Figure 1) is an interpolating vertex.

Now, we state the following lemma which gives a stability result of the cubic Scott-Vogelius pair. We refer to [17] for a detailed proof.

Lemma 3.9. *Suppose that $k = 3$ and $\mathcal{V}_h^I \subset \mathcal{L}_h$. Then there holds*

$$Y_h^{TH} \subset Q_h^{TH} := \nabla\cdot \boldsymbol{X}_h^{TH} = \{q \in \mathcal{P}_{k-1}(\mathcal{T}_h)\cap L_0^2(\Omega) : \sum_{\ell=1}^{M}(-1)^\ell q|_{T_\ell}(z) = 0\ \forall z \in \mathcal{S}_h\}.$$

Moreover, $\boldsymbol{X}_h^{TH} \times Q_h^{TH}$ represents an inf-sup stable pair with β_Q independent of size of the triangles in $\mathcal{T}_h$. Rather, $\beta_Q = C\Theta_*$ for some h-independent constant $C > 0$.

Combining Lemma 3.9 with Theorem 2.2 then yields the convergence of the grad-div stabilized Taylor–Hood pair.

Theorem 3.10. *Let $\{\gamma_i\}_{i=1}^\infty \subset \mathbb{R}$ with $\gamma_i \to \infty$ and $(\boldsymbol{u}_i, p_i) \in \boldsymbol{X}_h^{TH} \times Y_h^{TH}$ be the solution of the grad-div stabilized Stokes problem* (5) *corresponding to γ_i using the Taylor–Hood pair with $k = 3$. Assume $\mathcal{V}_h^I \subset \mathcal{L}_h$, i.e., all interior vertices in $\mathcal{T}_h$ are interpolating vertices. Then $\boldsymbol{u}_i \to \boldsymbol{w}_h$ and $p_i - \gamma_i\nabla\cdot\boldsymbol{u}_i \to p_h$ as $i \to \infty$ for some $\boldsymbol{w}_h \in \boldsymbol{X}_h^{TH} \cap \boldsymbol{V}$ and $p_h \in Q_h^{TH}$ with $(\boldsymbol{w}_h, p_h)$ being the solution for* (11) *with $\boldsymbol{X}_h \times Q_h = \boldsymbol{X}_h^{TH} \times Q_h^{TH}$. The convergence of $(\boldsymbol{u}_i, p_i - \gamma_i\nabla\cdot\boldsymbol{u}_i)$ satisfies* (19).

3.3. The Quadratic-Linear Taylor–Hood pair on Clough-Tocher splits. The case quadratic–linear Taylor–Hood pair on Clough-Tocher splits was discussed and studied in detail in [7]; here, we state these results for completeness.

A Clough–Tocher split (or refinement) of a shape–regular triangulation $\mathcal{T}_h$ is obtained connecting the vertices of each triangle $T \in \mathcal{T}_h$ to its barycenter. Thus, each triangle is split into three sub-triangles. Denote by $\mathcal{T}_h^{CT}$ the Clough-Tocher split of $\mathcal{T}_h$, and, with an abuse of notation, define the quadratic–linear Taylor–Hood pair on $\mathcal{T}_h^{CT}$:

$$\boldsymbol{X}_h^{TH} = \boldsymbol{\mathcal{P}}_2(\mathcal{T}_h^{CT}) \cap \boldsymbol{H}_0^1(\Omega), \tag{21a}$$

$$Y_h^{TH} = \mathcal{P}_1(\mathcal{T}_h^{CT}) \cap H^1(\Omega) \cap L_0^2(\Omega). \tag{21b}$$

The following lemma gives a characterization of the divergence acting on $\boldsymbol{X}_h^{TH}$ and states that the quadratic-linear Scott–Vogelius pair is stable on Clough–Tocher splits. Its proof can be found in [3, 14].

Lemma 3.11. *Let $\boldsymbol{X}_h^{TH} \times Y_h^{TH}$ be defined by* (21). *Then there holds*

$$Y_h^{TH} \subset Q_h^{TH} := \nabla\cdot\boldsymbol{X}_h^{TH} = \mathcal{P}_1(\mathcal{T}_h^{CT}) \cap L_0^2(\Omega).$$

Moreover, $\boldsymbol{X}_h^{TH} \times Q_h^{TH}$ represents an inf-sup stable pair with inf-sup constant β_Q independent of size of the triangles in $\mathcal{T}_h$.

Combining Lemma 3.11 with Theorem 2.2 then yields the convergence of the (low–order) grad-div stabilized Taylor–Hood pair.

Theorem 3.12. *Let $\boldsymbol{X}_h^{TH} \times Y_h^{TH}$ be defined by* (21), *and let $\{\gamma_i\}_{i=1}^\infty \subset \mathbb{R}$ with $\gamma_i \to \infty$. Let $(\boldsymbol{u}_i, p_i) \in \boldsymbol{X}_h^{TH} \times Y_h^{TH}$ be the solution of the grad-div stabilized Stokes problem* (5) *corresponding to γ_i. Then $\boldsymbol{u}_i \to \boldsymbol{w}_h$ and $p_i - \gamma_i\nabla\cdot\boldsymbol{u}_i \to p_h$ as $i \to \infty$ with rate $O(\gamma_i^{-1})$ for some $\boldsymbol{w}_h \in \boldsymbol{X}_h^{TH} \cap \boldsymbol{V}$ and $p_h \in Q_h^{TH}$ with $(\boldsymbol{w}_h, p_h)$ being the solution to* (11). *If $\boldsymbol{u} \in \boldsymbol{H}^s(\Omega)$ for some $s \ge 1$, then the divergence–free function $\boldsymbol{w}_h$ satisfies*

$$\|\nabla(\boldsymbol{u} - \boldsymbol{w}_h)\| \le Ch^{\ell-1}\|\boldsymbol{u}\|_{H^\ell(\Omega)}, \tag{22}$$

where $\ell = \min\{3, s\}$ and $C > 0$ is independent of h, γ, μ and β_Q.

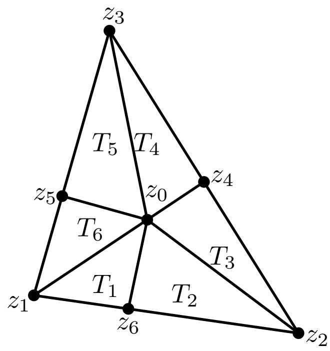

FIGURE 2. A Powell-Sabin local split of a triangle. Note that the vertices z_4, z_5, and z_6 are singular vertices in global mesh.

Proof. The convergence and convergence rates for the sequence $\{(\boldsymbol{u}_i, p_i - \gamma_i \nabla \cdot \boldsymbol{u}_i)\}_{i=1}^{\infty}$ directly follow from Lemma 3.3 with Theorem 2.2 (see also [7]).

To prove (22), and to show that the constant $C > 0$ is independent of β_Q, we first use the estimate (6):

$$\|\nabla(\boldsymbol{u} - \boldsymbol{w}_h)\| \le \inf_{\boldsymbol{v} \in \boldsymbol{V} \cap \boldsymbol{X}_h} \|\nabla(\boldsymbol{u} - \boldsymbol{v})\|.$$

Following the ideas in Theorem 3.4, we introduce the modified H^2-conforming Hsieh–Clough–Tocher finite element space [18]

$$\Sigma_h^{CT} = H_0^2(\Omega) \cap \mathcal{P}_3(\mathcal{T}_h^{CT}).$$

We then have [18]

$$\nabla \times \Sigma_h^{CT} := \{\nabla \times s : \ s \in \Sigma_h^{CT}\} \subset \boldsymbol{V} \cap \boldsymbol{X}_h.$$

Writing $\boldsymbol{u} = \nabla \times \psi$ for some $\psi \in H_0^2(\Omega) \cap H^{s+1}(\Omega)$, we have

$$\begin{aligned}\inf_{\boldsymbol{v} \in \boldsymbol{V} \cap \boldsymbol{X}_h} \|\nabla(\boldsymbol{u} - \boldsymbol{v})\| &\le \inf_{\boldsymbol{v} \in \nabla \times \Sigma_h^{CT}} \|\nabla(\boldsymbol{u} - \boldsymbol{v})\| \\ &= \inf_{s \in \Sigma_h^{CT}} \|D^2(\psi - s)\| \le C h^{\ell-1} \|\psi\|_{H^{\ell-1}(\Omega)} \le C h^{\ell-1} \|\boldsymbol{u}\|_{H^{\ell}(\Omega)}.\end{aligned}$$

□

4. Application II: The $\boldsymbol{\mathcal{P}}_1 \times \mathcal{P}_0$ pair on Powell-Sabin Splits

In the previous section, we considered the Taylor–Hood pair with grad-div stabilization for various polynomial degrees. The general theme in the arguments is to use the stability of the Scott–Vogelius pair to prove convergence and the absence of locking in the limiting case $\gamma \to \infty$. In this section, we show that the grad-div connection discussed in the previous sections can be generalized to the low–order $\boldsymbol{\mathcal{P}}_1 \times \mathcal{P}_0$ pair defined on a Powell-Sabin split mesh by incorporating the recently developed divergence–free methods in [15, 8].

As before, we start with a shape–regular simplicial triangulation $\mathcal{T}_h$ of Ω. We then construct the Powell–Sabin split of $\mathcal{T}_h$ as follows [25, 22]. Let $T \in \mathcal{T}_h$ be a triangle with vertices z_1, z_2 and z_3 labelled counterclockwise, and let z_0 be the incenter of T. Denote the edges of T by $\{e_i\}_{i=1}^3$, labelled such that z_i is not a vertex of e_i. Let z_{3+i} be the interior point of the edge of e_i that is the intersection of the line segment connecting the incenters of the triangles T and its neighboring triangle

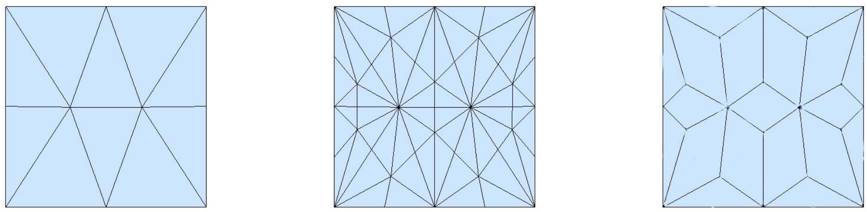

FIGURE 3. A triangulation $\mathcal{T}_h$ of the unit square (left), its Powell–Sabin refinement $\mathcal{T}_h^{PS}$ (middle), and the mesh $\mathcal{K}_h^{PS}$ (right).

that has e_i as an edge. We then construct the triangulation $T^{PS} = \{T_1, ..., T_6\}$ by connecting each z_i to z_0 for $1 \le i \le 6$; see Figures 2 and 3.

Let $\mathcal{T}_h^{PS} = \bigcup_{T\in\mathcal{T}_h} \bigcup_{\tau\in T^{PS}} \tau$ be the global triangulation of Ω, and $\mathcal{V}_h^{PS}$ be the set of vertices of $\mathcal{T}_h^{PS}$. Let $\mathcal{S}_h^{PS} \subset \mathcal{V}_h^{PS}$ be the set of all singular vertices in $\mathcal{T}_h^{PS}$. Let $\mathcal{S}_h^I = \{z \in \mathcal{S}_h^{PS} : z \notin \partial\Omega\}$ be the set of interior singular vertices, and $\mathcal{S}_h^B = \{z \in \mathcal{S}_h^{PS} : z \in \partial\Omega\}$ be the set of boundary singular vertices. Observe that each $z \in \mathcal{S}_h^I$ is attached to exactly four triangles, and each $z \in \mathcal{S}_h^B$ is attached to exactly two triangles. By construction, the cardinality of $\mathcal{S}_h^{PS}$ is exactly the number of edges in $\mathcal{T}_h$.

Definition 4.1. Let $p \in \mathcal{P}_0(\mathcal{T}_h^{PS}) = \{q \in L^2(\Omega) : q_{|T} \in P_0(T), \forall T \in \mathcal{T}_h^{PS}\}$. We say that p satisfies the *weak continuity property on $\mathcal{T}_h^{PS}$ if for any $z \in \mathcal{S}_h^I$ and $\{T_1, ..., T_4\} = \mathcal{T}_z \subset \mathcal{T}_h^{PS}$ we have that*

$$p_{|T_1} - p_{|T_2} + p_{|T_3} - p_{|T_4} = 0,$$

and for any $z \in \mathcal{S}_h^B$ and $\{T_1, T_2\} = \mathcal{T}_z \subset \mathcal{T}_h^{PS}$ we have that

$$p_{|T_1} = p_{|T_2}.$$

We introduce the finite element pair $\boldsymbol{X}_h^{PS} \times Q_h^{PS}$ defined on the Powell-Sabin triangulation $\mathcal{T}_h^{PS}$ proposed in [15]:

(23a) $\boldsymbol{X}_h^{PS} = \boldsymbol{\mathcal{P}}_1(\mathcal{T}_h^{PS}) \cap \boldsymbol{H}_0^1(\Omega),$

(23b) $Q_h^{PS} = \{q \in \mathcal{P}_0(\mathcal{T}_h^{PS}) \cap L_0^2(\Omega) :$ *q satisfies the weak continuity property*$\}.$

Now, we state the following lemma concerning the image of the divergence operator acting on $\boldsymbol{X}_h^{PS}$ and the inf-sup stability of $\boldsymbol{X}_h^{PS} \times Q_h^{PS}$. We refer to [15] for a detailed proof.

Lemma 4.2. *There holds*

$$\nabla \cdot \boldsymbol{X}_h^{PS} = Q_h^{PS}$$

with bounded right-inverse. Therefore, $\boldsymbol{X}_h^{PS} \times Q_h^{PS}$ is inf-sup stable, with inf-sup constant β_Q independent of h.

We note that, while $\boldsymbol{X}_h^{PS} \times Q_h^{PS}$ is an inf-sup stable and divergence–free pair, the construction of a basis for the pressure space and its implementation are non–trivial. Here, we propose a smaller and simpler pressure space that conforms to the framework in the previous sections. To this end, we let

$$\mathcal{K}_h^{PS} = \{ \bigcup_{T\in\mathcal{T}_z} T : z \in \mathcal{S}_h^{PS}\}$$

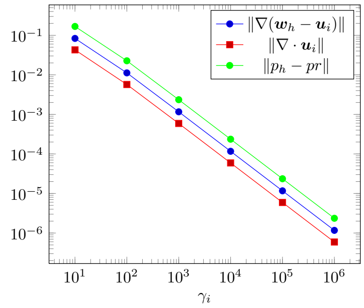

FIGURE 4. Numerical results on Powell-Sabin splits using the $\boldsymbol{\mathcal{P}}_1 \times \mathcal{P}_0$ pairs for fixed $h = 1/32$ and viscosity $\mu = 1$. Here, $pr = p_i - \gamma_i \nabla \cdot \boldsymbol{u}_i$. The plot shows $O(\gamma_i^{-1})$ convergence for all three quantities.

be the mesh obtained by connecting the triangles associated with each singular vertex. Thus, $\mathcal{K}_h^{PS}$ is a set consisting of quadrilaterals (in the case that z is an interior singular vertex) and triangles (in the case that z is a boundary singular vertex); see Figure 3.

We define the auxiliary pressure space

$$Y_h^{PS} = \{q \in L_0^2(\Omega) : q|_K \in P_0(K), \forall K \in \mathcal{K}_h^{PS}\}. \tag{24}$$

Remark 4.3. It was shown that the pair $\boldsymbol{X}_h^{PS} \times Q_h^{PS}$ is inf-sup stable when defined on the mesh $\mathcal{T}_h^{PS}$. Since $Y_h^{PS} \subset Q_h^{PS}$, the pair $\boldsymbol{X}_h^{PS} \times Y_h^{PS}$ is stable. Hence, we can incorporate Theorem 2.1 to conclude the following theorem.

Theorem 4.4. *Let $\{\gamma_i\}_{i=1}^{\infty} \subset \mathbb{R}$ with $\gamma_i \to \infty$ and $(\boldsymbol{u}_i, p_i) \in \boldsymbol{X}_h^{PS} \times Y_h^{PS}$ be the solution of the grad-div stabilized Stokes problem* (5) *correspondes to γ_i using the pair $\boldsymbol{X}_h^{PS} \times Y_h^{PS}$. Then $\boldsymbol{u}_i \to \boldsymbol{w}_h$ and $p_i - \gamma_i \nabla \cdot \boldsymbol{u}_i \to p_h$ as $i \to \infty$ with rate $O(\gamma_i^{-1})$ for some $\boldsymbol{w}_h \in \boldsymbol{X}_h^{PS} \cap \boldsymbol{V}$ and $p_h \in Q_h^{PS}$ with $(\boldsymbol{w}_h, p_h)$ being the solution for* (11) *with $\boldsymbol{X}_h \times Q_h = \boldsymbol{X}_h^{PS} \times Q_h^{PS}$.*

5. Numerical Examples

In this section, we perform some simple numerical experiments and compare the results with the theoretical ones given in the previous sections. In all tests, we take the domain to be the unit square $\Omega = (0,1)^2$, and choose the source function such that the exact velocity and pressure solutions are given respectively as

$$\boldsymbol{u} = \begin{pmatrix} \pi \sin^2(\pi x)\sin(2\pi y) \\ -\pi \sin^2(\pi y)\sin(2\pi x) \end{pmatrix}, \qquad p = \cos(\pi x)\cos(\pi y). \tag{25}$$

5.1. The $\boldsymbol{\mathcal{P}}_1 \times \mathcal{P}_0$ pair on Powell–Sabin Splits.

In this section, we report and discuss the numerical results for the $\boldsymbol{\mathcal{P}}_1 \times \mathcal{P}_0$ pair on Powell–Sabin splits.

Let $\mathcal{T}_h$ be a quasi–uniform Delaunay triangulation of Ω with $h = 1/32$, and let $\mathcal{T}_h^{PS}$ be the corresponding Powell-Sabin global triangulation (cf. Section 4). We compute problem (11) with $\boldsymbol{X}_h \times Q_h = \boldsymbol{X}_h^{PS} \times Q_h^{PS}$ defined by (23), and denote the solution pair by $(\boldsymbol{w}_h, p_h)$. We also compute problem (5) with $\boldsymbol{X}_h \times Y_h = \boldsymbol{X}_h^{PS} \times Y_h^{PS}$ (cf. (24)), and denote the solution pair corresponding to γ_i by $(\boldsymbol{u}_i, p_i)$. The grad-div parameters are taken to be $\gamma_i = 10^i$ for $i = 1, \ldots, 6$.

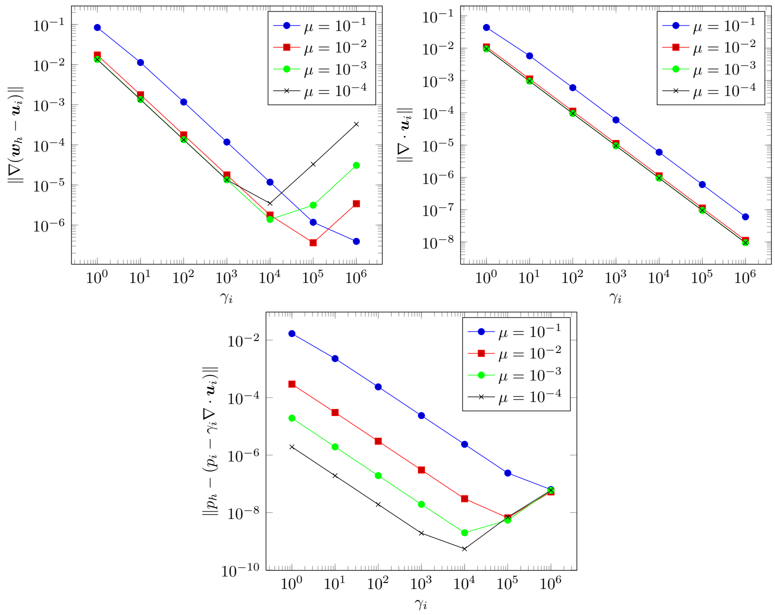

FIGURE 5. Numerical experiments using the $\boldsymbol{\mathcal{P}}_1 \times \mathcal{P}_0$ pairs on Powell–Sabin splits with fixed $h = 1/32$ and varying viscosity μ. Here, $pr = p_i - \gamma_i \nabla \cdot \boldsymbol{u}_i$. The plot shows $O(\gamma_i^{-1})$ convergence for all three quantities. The increase in the first and third plots for large values of γ_i is due to round–off error.

5.1.1. The $\boldsymbol{\mathcal{P}}_1 \times \mathcal{P}_0$ pair on Powell-Sabin Splits with fixed viscosity $\mu = 1$. In Figure 4, we plot the quantities $\|\nabla(\boldsymbol{w}_h - \boldsymbol{u}_i)\|$,$\|\nabla \cdot \boldsymbol{u}_i\|$ and $\|p_h - (p_i - \gamma_i \nabla \cdot \boldsymbol{u}_i)\|$ versus γ_i for fixed $h = 1/32$ and fixed viscosity $\mu = 1$. The plot clearly shows linear convergence with respect to γ_i^{-1} for all three quantities, which is in exact agreement with Theorem 4.4.

5.1.2. The $\boldsymbol{\mathcal{P}}_1 \times \mathcal{P}_0$ pair on Powell-Sabin Splits with varying viscosity. In these series of tests, we compute the same problem as the previous section, but for different viscosity values: $\mu = 10^{-j}$ for $j = 1, 2, 3, 4$. We report the differences $\|\nabla(\boldsymbol{w}_h - \boldsymbol{u}_i)\|$,$\|\nabla \cdot \boldsymbol{u}_i\|$ and $\|p_h - (p_i - \gamma_i \nabla \cdot \boldsymbol{u}_i)\|$ versus the grad-div parameter in Figure 5.

Again, we observe that all three quantities converge with rate $O(\gamma_i^{-1})$ for each value of μ, at least for moderately sized values of γ_i. On the other hand, we see that, for small values of μ, the differences $\|p_h - (p_i - g\nabla \cdot \boldsymbol{u}_i)\|_{L^2(\Omega)}$ and $\|\nabla(\boldsymbol{w}_h - \boldsymbol{u}_i)\|_{L^2(\Omega)}$ increase (with rate $= O(\gamma_i)$) as $\gamma_i \to \infty$. This behavior is due to round-off error as we now explain.

Observe that (14) reads

$$\mu(\nabla \boldsymbol{e}_i, \nabla \boldsymbol{v}) - (p_h - p_i, \nabla \cdot \boldsymbol{v}) + \gamma_i(\nabla \cdot \boldsymbol{e}_i, \nabla \cdot \boldsymbol{v}) = 0 \qquad \forall \boldsymbol{v} \in \boldsymbol{X}_h,$$

where $\boldsymbol{e}_i = \boldsymbol{w}_h - \boldsymbol{u}_i$. Consequently, by setting $\boldsymbol{v} = \boldsymbol{e}_i$ and using $\nabla \cdot \boldsymbol{w}_h = 0$, and dividing by μ and rearrange terms, we find

$$\|\nabla(\boldsymbol{w}_h - \boldsymbol{u}_i)\|^2_{L^2(\Omega)} = \|\nabla \boldsymbol{e}_i\|^2 = \frac{1}{\mu}(p_h - (p_i - \gamma_i \nabla \cdot \boldsymbol{u}_i), \nabla \cdot \boldsymbol{u}_i).$$

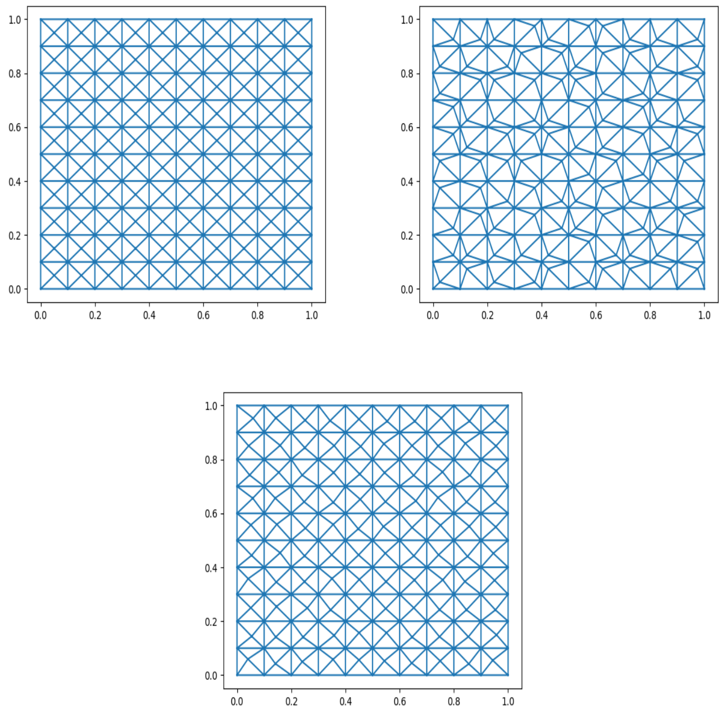

FIGURE 6. A criss–cross mesh of the unit square with $h = 1/10$ (left), and its perturbations with $\alpha = 0$ (middle) and $\alpha = 1$ (right).

We computed the term $\frac{1}{\mu}(p_h - (p_i - \gamma_i \nabla \cdot \boldsymbol{u}_i), \nabla \cdot \boldsymbol{u}_i)$, and we observed that as soon as this term is less than machine epsilon, both quantities $\|\nabla(\boldsymbol{w}_h - \boldsymbol{u}_i)\|$ and $\|p_h - (p_i - \gamma_i \nabla \cdot \boldsymbol{u}_i)\|$ grow as $\gamma_i \to \infty$.

5.2. Taylor–Hood Finite Elements. In this section we report and discuss the numerical results for Taylor–Hood finite element with polynomial degrees $k = 4, 3, 2$, and compare the results with the theoretical ones established in Section 3. We compute problem (11) with $\boldsymbol{X}_h \times Q_h = \boldsymbol{X}_h^{TH} \times Q_h^{TH}$, and we denote the solution pair by $(\boldsymbol{w}_h, p_h)$. Also, we consider the problem (5) with $\boldsymbol{X}_h \times Y_h = \boldsymbol{X}_h^{TH} \times Y_h^{TH}$ and we denote the solution pair by $(\boldsymbol{u}_i, p_i)$ that corresponding to γ_i.

5.2.1. Grad-div Taylor–Hood methods on perturbed criss–cross meshes with fixed viscosity. Recall from Lemmas 3.3 and 3.9 that the stability of Scott–Vogelius pair depends on the vertex singularity of the mesh Θ_* given in Definition 3.1. This in turn affects the convergence behavior of the grad-div solution $(\boldsymbol{u}_i, p_i)$ to the divergence–free solution $(\boldsymbol{w}_h, p_h)$; see Theorems 3.4 and 3.10. The purpose of the tests presented in this section is to gauge the affect of the vertex singularity of the mesh, and to compare the numerical results with the theoretical ones derived in Section 3.

To this end, we start by constructing criss–cross triangulation of Ω with $h = 1/20$ which has $O(h^{-2})$ singular vertices. Then for each singular vertex of the

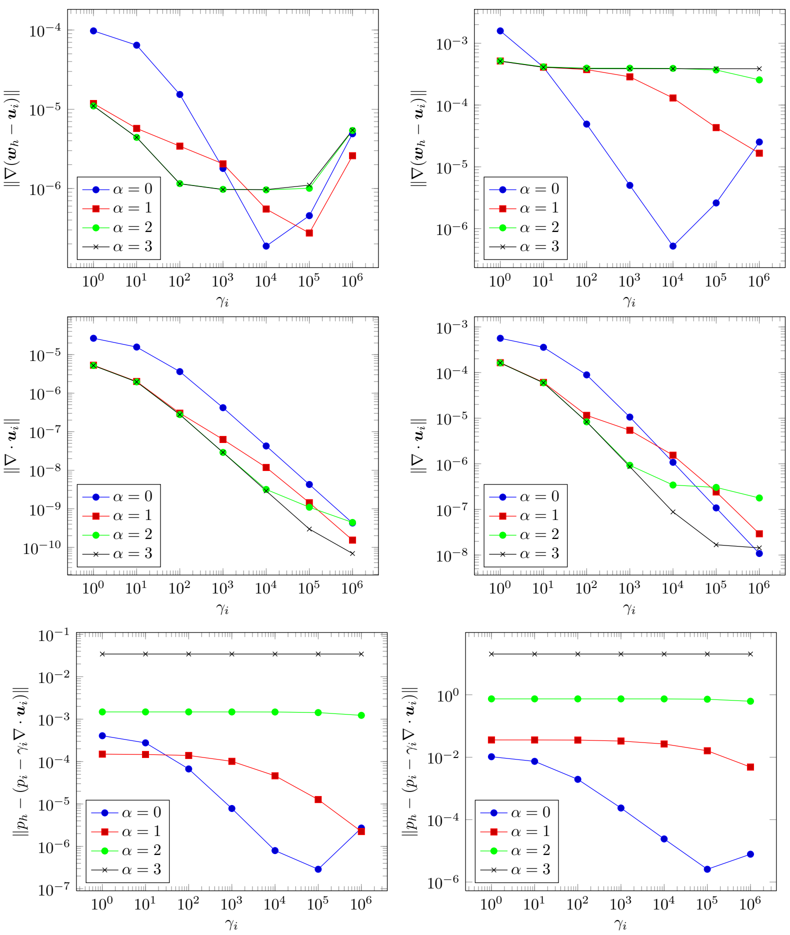

FIGURE 7. Results of the grad-div stabilized $\boldsymbol{\mathcal{P}}_k \times \mathcal{P}_{k-1}$ Taylor–Hood pair on $O(h^{\alpha+1})$ perturbed criss-cross meshes with $h = 1/20$ and $\mu = 1$. Left: $k = 4$. Right: $k = 3$.

triangulation, we add its coordinates by $(r_1, r_2)h^{\alpha+1}$, where $r_i \in \{-2, -1, 1, 2\}$ is chosen randomly, and with exponent $\alpha \in \{0, 1, 2, 3\}$; see Figure 6. The resulting perturbed mesh has no singular vertices, but simple trigonometric arguments show the vertex singularity of the mesh is $\Theta_* \approx h^\alpha$.

We report the quantities quantities $\|\nabla \cdot \boldsymbol{u}_i\|$, $\|\nabla(\boldsymbol{w}_h - \boldsymbol{u}_i)\|$, and $\|p_h - (p_i - \gamma_i \nabla \cdot \boldsymbol{u}_i)\|$ using the $\boldsymbol{\mathcal{P}}_k \times \boldsymbol{\mathcal{P}}_{k-1}$ $(k = 3, 4)$ Taylor–Hood and Scott–Vogelius elements with $\mu = 1$ in Figure 7. For comparison, the convergence estimate for the Taylor–Hood element stated in Theorems 3.4 and 3.10 read

$$h^\alpha \|p_h - (p_i - \gamma_i \nabla \cdot \boldsymbol{u}_i)\| \leq \|\nabla(\boldsymbol{w}_h - \boldsymbol{u}_i)\| \leq Ch^{-\alpha} \min\{h^{-\alpha}\gamma_i^{-1}, \gamma_i^{-1/2}\},$$

which suggests a deterioration of the "errors" for large perturbation exponents α. Indeed, Figure 7 shows pre-asymptotic $O(\gamma_i^{-1/2})$ convergence rates for $\alpha = 0$ before achieving $O(\gamma_i^{-1})$ rates for large values of γ_i. On the other hand, for larger α-values (e.g., $\alpha = 2, 3$), we see pre-asymptotic convergence $(k = 4)$ or no convergence $(k = 3)$. The deterioration of the errors for large α-values is most evident for the

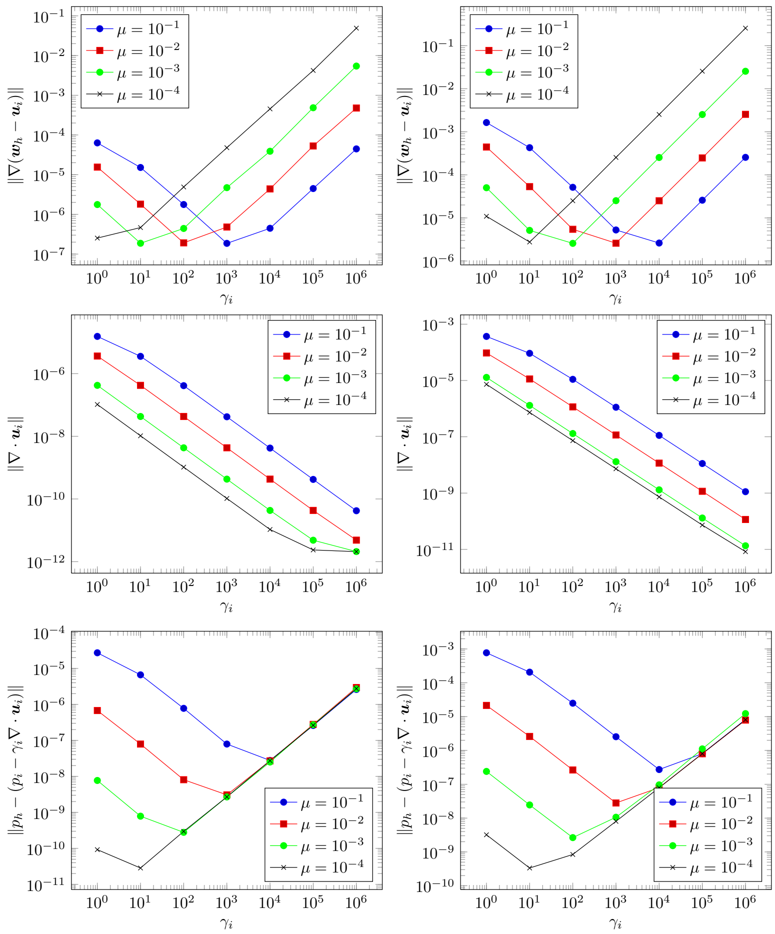

FIGURE 8. $\boldsymbol{\mathcal{P}}_k \times \mathcal{P}_{k-1}$ grad-div sequences errors for $O(h)$ perturbed mesh with different viscosities. Left: $k = 4$. Right: $k = 3$.

modified pressure, where Figure 7 shows no convergence with respect to γ_i for $\alpha \in \{2, 3\}$. Therefore we conclude from these results that the quantity Θ_* stated in Theorem 3.4 does influence the convergence of the grad-div solution.

On the other hand, Figure 7 shows $\|\nabla \cdot \boldsymbol{u}_i\| = O(\gamma_i^{-1})$ for any value α. Consequently, the convergence estimate of this quantity stated in Theorem 3.4 may not be sharp for this quantity.

5.2.2. Grad-div Taylor–Hood methods with varying viscosity. In this series of tests we compute the grad-div Taylor–Hood method with $k = 3, 4$ and vary the viscosity $\mu = 10^{-j}$ $j = 1, 2, 3, 4$ on a perturbed criss cross mesh with $h = 1/20$ and $\alpha = 0$. In this setting, vertex singularity of the mesh is $\Theta_* = O(1)$. The estimates stated in Theorems 3.4 and 3.10 read

$$\mu^{-1}\|p_h - (p_i - \gamma_i \nabla \cdot \boldsymbol{u}_i)\| \leq \|\nabla(\boldsymbol{w}_h - \boldsymbol{u}_i)\| \leq C \min\{\gamma_i^{-1}, (\mu\gamma_i)^{-1/2}\}.$$

We report the quantities $\|\nabla(\boldsymbol{w} - \boldsymbol{u}_i)\|$, $\|\nabla \cdot \boldsymbol{u}_i\|$ and $\|p_h - (p_i - \gamma_i \nabla \cdot \boldsymbol{u}_i)\|$ for $\gamma_i = 10^i$ and $k \in \{3, 4\}$ in Figure 8. We observe that the estimate $\|\nabla \cdot \boldsymbol{u}_i\|$ converges with rate $O(\gamma_i^{-1})$ regardless of the value of μ. The errors $\|p_h - (p_i - \gamma_i \nabla \cdot \boldsymbol{u}_i)\|$ and

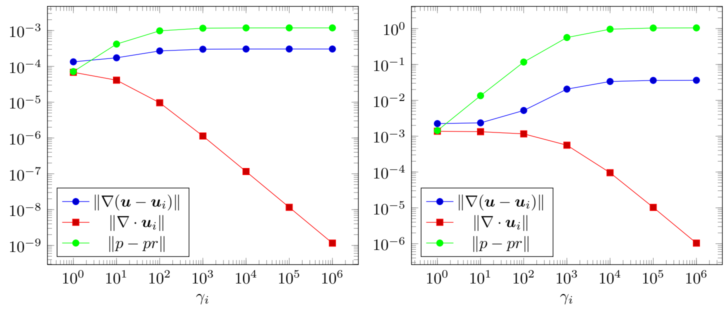

FIGURE 9. Errors of grad-div finite element method using the Taylor-Hood pair $\boldsymbol{\mathcal{P}}_k \times \mathcal{P}_{k-1}$ on type–I triangulation with $k = 4$ (left) and $k = 3$ (right). Here, $pr = p_i - \gamma_i \nabla \cdot \boldsymbol{u}_i$.

.

$\|\nabla(\boldsymbol{w}_h - \boldsymbol{u}_i)\|$ initially converge with rates $O(\gamma_i^{-1})$ but quickly increase for large γ_i-values with rate $O(\gamma_i)$ due to the round-off error (cf. Section 5.1.2).

5.3. Grad-div Taylor–Hood methods on type–I triangulations. In the final set of numerical experiments, we compute the grad-div Taylor–Hood methods on type–I triangulations with $h = 1/24$ (cf. Figure 1). Recall from Remark 3.8 that on this mesh, not all interior vertices are interpolating vertices, and therefore the cubic–quadratic Scott–Vogelius pair is not stable on this mesh.

Similar to the previous sections with compute the grad-div stabilized finite element method using the $\boldsymbol{\mathcal{P}}_k \times \mathcal{P}_{k-1}$ pair with $k = 3, 4$ and fixed viscosity $\mu = 1$. As the Scott–Vogelius pair $(\boldsymbol{w}_h, p_h)$ is unavailable on this mesh, we instead compute the errors $\|\nabla(\boldsymbol{u} - \boldsymbol{u}_i)\|$, $\|\nabla \cdot \boldsymbol{u}_i\|$, and $\|p - (p_i - \gamma_i \nabla \cdot \boldsymbol{u}_i)\|$, where $(\boldsymbol{u}, p)$ are given by (25).

We report these quantities in Figure 9. We observe a clear convergence of the divergence of the computed solution with $\|\nabla \cdot \boldsymbol{u}_i\| = O(\gamma_i^{-1})$ (asymptotically) in both cases $k = 3, 4$. On the other hand, the errors for the quartic–cubic pair perform much better for large values of the grad-div parameter γ_i. Indeed, in this case the errors stabilize relatively quickly at $\gamma_i = 10^2$. On the other hand, for the cubic-quadratic case, we see that the errors $\|\nabla(\boldsymbol{u} - \boldsymbol{u}_i)\|$ and especially $\|p - (p_i - \gamma_i \nabla \cdot \boldsymbol{u}_i)\|$ increase for large γ_i-values. This behavior may be due to the instability of the Scott-Vogelius pair and the lack of a discrete divergence–free subspace with optimal approximation properties.

Acknowledgments

This work is supported in part by NSF grants DMS-1719829 and DMS-2011733.

References

[1] N .Ahmed, On the grad-div stabilization for the steady Oseen and Navier-Stokes equations, Calcolo, 54(1):471–501, 2017.

[2] J. H. Argyris, I. Fried, D. W. Scharpf The TUBA family of plate elements for the matrix displacement method, Aero. J. Roy. Aero. Soc., 72:701–709, 1968.

[3] D.N. Arnold and J. Qin, Quadratic velocity/linear pressure Stokes elements, in Advances in Computer Methods for Partial Differential Equations VII, ed. R. Vichnevetsky and R.S. Steplemen, 1992.

[4] M. Braack, E. Burman, V. John, and G. Lube, Stabilized finite element methods for the generalized Oseen problem, Comput. Methods Appl. Mech. Engrg., 196(4-6):853–866, 2007.

[5] D. Boffi, F. Brezzi and M. Fortin, Finite elements for the Stokes problem, in Mixed Finite Elements, Compatibility Conditions, and Applications, Lectures given at the C.I.M.E. Summer School, Springer-Verlag, Berlin, 2008.
[6] S. C. Brenner, L. R. Scott, The Mathematical Theory of Finite Element Methods, Third Edition, Springer, 2000.
[7] M. A. Case, V. J. Ervin, A. Linke, L. G. Rebholz Connection between Scott–Voglius and Grad-Div stabilized Taylor–Hood FE approximations of the Navier–Stokes equations, SIAM J. Numer. Anal., 49(4):1461–1481, 2011.
[8] S. Christiansen and K. Hu, Generalized finite element systems for smooth differential forms and Stokes' problem, Numer. Math., DOI:10.1007/s00211-018-0970-6, 2018.
[9] J. de Frutos, B. Garcia-Archilla, V. John, and J. Novo, Grad-div stabilization for the evolutionary Oseen problem with inf-sup stable finite elements, J. Sci. Comput., 66(3):991–1024, 2016.
[10] J. de Frutos, B. Garcia-Archilla, V. John, and J. Novo, Analysis of the grad-div stabilization for the time-dependent Navier-Stokes equations with inf-sup stable finite elements, Adv. Comput. Math., 44(1):195–225, 2018.
[11] R.S. Falk, M. Neilan, Stokes complexes and the construction of stable finite elements with pointwise mass conservation, SIAM J. Numer. Anal., 51(2):1308–1326, 2013.
[12] K. J. Galvin, A. Linke, L. G. Rebholz, N. E. Wilson, Stabilizing poor mass conservation in incompressible ow problems with large irrotational forcing and application to thermal convection, Comput. Methods Appl. Mech. Engrg., 237/240 (2012), pp. 166-176,
[13] V. Girault, P.-A Raviart, Finite element methods for Navier-Stokes equations. Theory and algorithms. Springer Series in Computational Mathematics, 5. Springer-Verlag, Berlin, 1986.
[14] J. Guzmán and M. Neilan, Inf-sup stable finite elements on barycentric refinements producing divergence–free approximations in arbitrary dimension, SIAM J. Numer. Anal., 56(5):2826–2844, 2018.
[15] J. Guzman, A. Lischke, M. Neilan Exact Sequences on Powell-Sabin Split, Calcolo, to appear.
[16] J. Guzman, R. Scott, The Scott-Vogelius Finite Element revisited, Math. Comp., 88(316):515–529, 2019.
[17] J. Guzman, R. Scott, Cubic Lagrange elements satisfying exact incompressibility, SMAI J. Comput. Math. 4:345–374, 2018.
[18] V. John, A. Linke, C. Merdon, M. Neilan, and L.G. Rebholz, On the divergence constraint in mixed finite element methods for incompressible flows, SIAM Rev., 59(3):492–544, 2017.
[19] A. Linke, L.G. Rebholz, and N.E. Wilson, On the convergence rate of grad-div stabilized Taylor-Hood to Scott-Vogelius solutions for incompressible flow problems, J. Math. Anal. Appl., 381(2):612–626, 2011.
[20] A. Linke, M. Neilan, L.G. Rebholz, and N.E. Wilson, A connection between coupled penalty projection timestepping schemes with FE spatial discretization for the Naiver-Stokes equations, J. Numer. Math., 25(4):229–248, 2017.
[21] G. Lube and M. A. Olshanskii, Stable finite-element calculation of incompressible flows using the rotation form of convection, IMA J. Numer. Anal., 22(3):437–461, 2002.
[22] M.-J. Lai and L. L. Schumaker, Spline functions on triangulations, Encyclopedia of Mathematics and its Applications, 110., Cambridge University Press, Cambridge, 2007.
[23] M. Olshanskii and A. Reusken, Grad-div stabilization for Stokes equations, Math. Comp., 73:1699–1718, 2004.
[24] M. Olshanskii, G. Lube, T. Heister, and J. Löwe Grad-div stabilization and subgrid pressure models for the incompressible Navier-Stokes equations, Comput. Methods Appl. Mech. Engrg., 198(49–52):3975–3988, 2009.
[25] M. J. D. Powell and M. A. Sabin, Piecewise quadratic approximations on triangles, ACM Trans. Math. Software 3(4):316–325, 1977.
[26] L. R. Scott, M. Vogelius, Conforming finite element methods for incompressible and nearly incompressible continua, in Large-Scale Computations in Fluid Mechanics, Part 2. Lectures in Appl. Math. 22-2, Amer. Math. Soc., Providence, RI, 1985, pp. 221244.
[27] E.W. Jenkins, V. John, A. Linke, L. G. Rebholz On the parameter choice in grad-div stabilization for the Stokes equations, Adv Comput Math (2014) 40:491516.

Department of Mathematics, University of Pittsburgh, Pittsburgh, PA 15260
E-mail: `neilan@pitt.edu and AMZ56@pitt.edu`